Combined state and parameter estimation for a landslide model using Kalman filter

Mohit Mishra, Gildas Besancon, Guillaume Chambon, Laurent Baillet

Combined state and parameter estimation for a landslide model using Kalman filter

Mohit Mishra [*], **Gildas Besançon** [*], **Guillaume Chambon** [**], **Laurent Baillet** [***]

[*] *Univ. Grenoble Alpes, CNRS, Grenoble INP - Institute of Engineering, GIPSA-lab, 38000 Grenoble, France (e-mail: [mohit.mishra, gildas.besancon]@gipsa-lab.grenoble-inp.fr)*
[**] *Univ. Grenoble Alpes, INRAE, UR ETGR, Grenoble, France (e-mail: guillaume.chambon@inrae.fr)*
[***] *Univ. Grenoble Alpes, CNRS, ISTerre, Grenoble, France (e-mail: laurent.baillet@univ-grenoble-alpes.fr)*

Abstract: The paper presents a combined state and parameter estimation for a landslide model using a Kalman filter. The model under investigation is based on underlying mechanics that depicts a landslide behavior. This system is described by an Ordinary Differential Equation (ODE) with displacement as a state and landslide geometrical and material properties as parameters. The Kalman filter approach is utilized on a simplified model equation for state and parameter estimation. Finally, the presented approach is validated by two illustrative examples, the first one a synthetic case study and the second one on Super-Sauze landslide data taken from the literature.

Keywords: State estimation, parameter estimation, Kalman filter, landslide model, Super-Sauze landslide.

1. INTRODUCTION

Landslide is a gravitational hazard causing substantial cost in life losses and damaging infrastructure worldwide each year. Most of the landslides are triggered by heavy precipitation; earthquakes and human activities such as construction work can be other reasons. Avoiding building infrastructure near or on the exposed zone is a suitable strategy in landslide risk management, while stabilizing unstable slopes and installing protecting structures are some of the other available options. However, with rapid urbanization, infrastructures are still being constructed in a landslide-prone zone (Nyambod, 2010). The implementation of Early Warning Systems (EWS) can help take timely actions to reduce life and economic losses (Krøgli et al., 2018). These EWS's use specific monitoring strategies that assess the environment's current status and determine trends in environmental parameters to generate accurate warnings.

Some of the landslide EWS works on a rainfall threshold approach to establish a trend between movement and the triggering precipitation from past data. As this critical value of precipitation is defined on statistical and experience bases, this approach often provides false alarms (Guzzetti et al., 2007). One of the perspective approaches is based on seismic measurements, in which seismic parameters are derived from monitoring that provides a significant precursory signal (Fiolleau et al., 2020). Another approach of landslide forecasting makes use of monitoring displacement (or velocity). This approach generates warning based on a change in slope displacement rates over time, e.g., inverse velocity criteria (Petley et al., 2005). Sometimes these warnings provide less reaction time to take necessary precautionary measures. Therefore, this approach can be enhanced by utilizing physics-based landslide models, e.g., sliding-consolidation model (Hutchinson, 1986), viscoplastic sliding-consolidation model (Corominas et al., 2005; Herrera et al., 2013; Bernardie et al., 2014) and extended sliding-consolidation model (Iverson, 2005) to predict future displacement/velocity. A similar approach has already been studied in (Corominas et al., 2005; Herrera et al., 2013; Bernardie et al., 2014). These models are sensitive to the initial conditions, parameter values, and input to the model, i.e., rainfall, water table height, or pore water pressure time-series. In this context, an additional interesting approach could be to analyze the changes in mechanical properties of the material (parameters) prior to events.

This paper presents combined state and parameter estimation for a simplified viscoplastic sliding model of a landslide. This system is described by an ODE with displacement as a state and landslide geometrical and material properties as parameters. The model is further simplified so as to apply Kalman filter approach to estimate displacement and unknown parameters (material properties, e.g., friction angle and viscosity). Finally, two illustrative examples validate the presented approach on two different cases: i) synthetic test case and ii) Super-Sauze landslide data taken from the literature (Bernardie et al., 2014). A similar perspective of displacement and

⋆ This work is supported by the French National Research Agency in the framework of the Investissements d'Avenir program (ANR-15-IDEX-02)

parameter estimation on the Super-Sauze landslide is studied in (Bernardie et al., 2014) using sequential quadratic programming (SQP) algorithm. For the extended sliding-consolidation model of a landslide, observer problems are solved by adjoint method (Mishra et al., 2020b) and observer design (Mishra et al., 2020a) on synthetically generated noisy data. Kalman filter-based estimation approach demonstrated its effectiveness in many studies and applications, for instance, state and parameter estimation in linear lung model (Saatci and Akan, 2009), lithium-ion battery (Meng et al., 2020), and asynchronous motors (Ţiclea and Besançon, 2006; Atkinson et al., 1991).

The paper's structure is as follows: A landslide model depicting landslide dynamics, and the problem statement is given in Section 2. Section 3 presents the proposed solution method. In Section 4, simulation results demonstrate the effectiveness of the proposed approach. Finally, some conclusions and future directions of the work are discussed in Section 5.

2. PROBLEM FORMULATION

2.1 Simplified viscoplastic sliding model

The viscoplastic sliding model (Corominas et al., 2005; Herrera et al., 2013; Bernardie et al., 2014) of a landslide assumes a slide block overlying thin shear zone, as shown in Fig. 1. Net destabilizing inertial force F_{di} is given by

$$F_{di} = \rho H A a(t) = F_g + F_r + F_c + F_p + F_v \tag{1}$$

where ρ is the soil density, H is the slide block height, A is the slide block base area, $a(t)$ is acceleration of the slide block, F_g is gravity imposed driving force ($F_g = \rho H A g \sin\theta$), F_r is basal Coulomb friction force ($F_r = -\rho H A g \cos\theta \tan\phi$), F_c is cohesive force ($F_c = -CA$), F_p is fricion force due to pore pressure ($F_p = p(t) A \tan\phi$), F_v is viscous force ($F_v = -\eta v(t) A / s_t$), g is the acceleration due to gravity, θ is the inclination angle, ϕ is the friction angle, C is the cohesion, $p(t)$ is pore water pressure at time t, η is the viscosity, $v(t)$ is velocity of the slide block, and s_t is the basal shear zone thickness.

The dimensional analysis shows that the inertia term $\rho H A a(t)$ is expected to remain much smaller than the other terms (i.e., steady-state is indeed reach very fast), so this term assumed to be null. Also, with the assumptions of a groundwater flow parallel to the slope surface, the pore water pressure is defined by

$$p(t) = \rho_w g \cos^2\theta w_t(t) \tag{2}$$

where ρ_w is the pore water density and $w_t(t)$ is water table height as shown in Fig. 1. Therefore, ignoring the inertia term, substituting F_g, F_r, F_c, F_p, F_v and (2) in (1), and rearranging the equation leads to dynamics

$$\begin{aligned}\dot{d} = v(t) = &\left(\frac{\rho}{\eta}\right) s_t H g sin\theta - \left(\frac{\rho tan\phi}{\eta}\right) s_t H g cos\theta \\ &- \left(\frac{1}{\eta}\right) s_t C + \left(\frac{tan\phi}{\eta}\right) s_t \rho_w g cos^2\theta w_t(t)\end{aligned} \tag{3}$$

where d is displacement of the slide block.

Notice that the upslope motion of the slide block is physically impossible, i.e., the slide block velocity can not be negative ($\dot{d} = v(t) \not< 0$). Such a situation arises

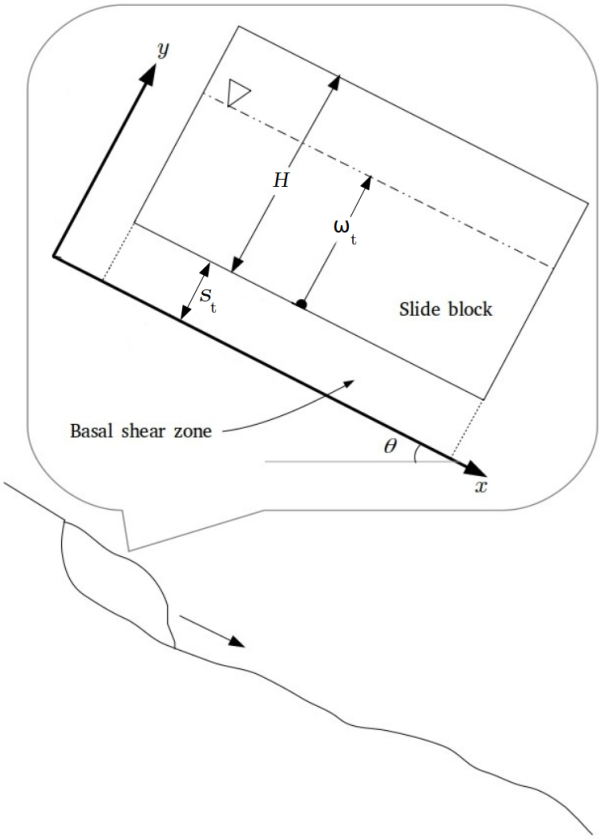

Fig. 1. Geometrical variables of the slide block

whenever water table height goes below critical water table height w_t^{crit}. The value of w_t^{crit} is evaluated as (derived from $\dot{d} = v(t) = 0$)

$$w_t^{crit} = \frac{C - \rho H g \sin\theta + \rho H g \cos\theta \tan\phi}{\rho_w g \cos^2\theta \tan\phi}. \tag{4}$$

Thus, when $w_t(t) \leq w_t^{crit}$ landslide obeys following dynamics

$$\dot{d} = v(t) = 0. \tag{5}$$

Therefore, the combined dynamics of the landslide is represented as

$$\dot{d} = \begin{cases} \left(\frac{\rho}{\eta}\right) s_t H g sin\theta - \left(\frac{\rho tan\phi}{\eta}\right) s_t H g cos\theta \\ - \left(\frac{1}{\eta}\right) s_t C + \left(\frac{tan\phi}{\eta}\right) s_t \rho_w g cos^2\theta w_t(t), & \text{if } w_t(t) > w_t^{crit} \\ 0, & \text{otherwise.} \end{cases} \tag{6}$$

Based on the model (6), this paper's primary goal is to estimate displacement d and unknown parameters from available measurements d_{mea}, known parameters and input $w_t(t)$. In most cases, geometrical parameters (H,θ,s_t) could be well known while few of the material properties, for instance, friction angle ϕ and viscosity η need to be estimated. Notice that model switches when $w_t(t) \leq w_t^{crit}$, therefore it is required to estimate w_t^{crit} which itself depends on parameter values in the estimation scheme.

Note: In the formulated problem, water table height $w_t(t)$ acts as an input, which is assumed to be known. In many scenarios, instead of $w_t(t)$, pore water pressure measurements could be available, and in such a situation $w_t(t)$ can be reconstructed from $p(t)$ using (2).

3. KALMAN FILTER BASED STATE AND PARAMETER ESTIMATION

In order to address the defined problem, let us first normalize parameters, by introducing a scaling factor $\bar{\eta}$ in equation (3) as follows:

$$\begin{aligned}\bar{\eta}\dot{d} = &\left(\frac{\bar{\eta}}{\eta}\right) s_t \rho H g sin\theta - \left(\frac{\bar{\eta} tan\phi}{\eta}\right) s_t \rho H g cos\theta \\ &- \left(\frac{\bar{\eta}}{\eta}\right) s_t C + \left(\frac{\bar{\eta} tan\phi}{\eta}\right) s_t \rho_w g cos^2\theta w_t(t).\end{aligned} \tag{7}$$

Now considering that η and ϕ are the parameters to be identified, the other ones being known, let us set:

$$\begin{bmatrix}\theta_1 \\ \theta_2\end{bmatrix} = s_t \begin{bmatrix}\rho H g \sin\theta - C & -\rho H g \cos\theta \\ 0 & \rho_w g cos^2\theta\end{bmatrix} \begin{bmatrix}\bar{\eta}/\eta \\ \bar{\eta}\tan\phi/\eta\end{bmatrix}. \tag{8}$$

Substituting (8) in (7), the model can then be extended by two state varaiables θ_1, θ_2 with $\dot{\theta}_1 = \dot{\theta}_2 = 0$. Taking into account w_t^{crit} it reads:

$$\begin{aligned}\dot{d} &= \begin{cases}\frac{\theta_1}{\bar{\eta}} + \frac{\theta_2}{\bar{\eta}} w_t(t) & \text{if } w_t(t) > w_t^{crit} \\ 0 & \text{otherwise}\end{cases} \\ \dot{\theta}_1 &= 0 \\ \dot{\theta}_2 &= 0.\end{aligned} \tag{9}$$

Owing to discrete measurements, let us write the system dynamics in discrete time,

$$\begin{bmatrix}d^{k+1} \\ \theta_1^{k+1} \\ \theta_2^{k+1}\end{bmatrix} = \begin{cases}\overbrace{\begin{bmatrix}1 & \frac{dt}{\bar{\eta}} & \frac{dt}{\bar{\eta}} w_t^k \\ 0 & 1 & 0 \\ 0 & 0 & 1\end{bmatrix}}^{\bar{A}_1^k} \begin{bmatrix}d^k \\ \theta_1^k \\ \theta_2^k\end{bmatrix}, & \text{if } w_t^k > w_t^{crit} \\ \underbrace{\begin{bmatrix}1 & 0 & 0 \\ 0 & 1 & 0 \\ 0 & 0 & 1\end{bmatrix}}_{\bar{A}_2^k} \begin{bmatrix}d^k \\ \theta_1^k \\ \theta_2^k\end{bmatrix}, & \text{otherwise}\end{cases} \tag{10}$$

where dt is the discrete time step, and the measurement is

$$y^k = d_{mea}^k = \bar{C}\left[d^k \ \theta_1^k \ \theta_2^k\right]^\intercal + v^k \tag{11}$$

where $\bar{C} = [1\ 0\ 0]$ and v^k denotes some measurement noise.

For dynamics (10)-(11), Kalman filter (Anderson and Moore, 1979) provide estimates of $\hat{d}$, $\hat{\theta}_1$ and $\hat{\theta}_2$ (see also (Ţiclea and Besançon, 2009) for a version with forgetting factor). Based on these estimates at each time step firstly $\bar{\eta}/\hat{\eta}$ and $\bar{\eta}\tan\hat{\phi}/\hat{\eta}$ are reconstructed using (8)

$$\begin{bmatrix}\bar{\eta}/\hat{\eta} \\ \bar{\eta}\tan\hat{\phi}/\hat{\eta}\end{bmatrix} = \frac{1}{s_t} \begin{bmatrix}\rho H g \sin\theta - C & -\rho H g \cos\theta \\ 0 & \rho_w g cos^2\theta\end{bmatrix}^{-1} \begin{bmatrix}\hat{\theta}_1 \\ \hat{\theta}_2\end{bmatrix}, \tag{12}$$

followed by

$$\hat{\eta} = \frac{\bar{\eta}}{[\bar{\eta}/\hat{\eta}]} \tag{13}$$

and

$$\hat{\phi} = \tan^{-1}\left(\left[\bar{\eta}\tan\hat{\phi}/\hat{\eta}\right] \times \frac{\hat{\eta}}{\bar{\eta}}\right). \tag{14}$$

In the proposed estimation scheme w_t^{crit} plays an important role, which depends on the parameter values, therefore at each step it is estimated as

$$\hat{w}_t^{crit} = \frac{C - \rho H g \sin\theta + \rho H g \cos\theta \tan\hat{\phi}}{\rho_w g \cos^2\theta \tan\hat{\phi}}. \tag{15}$$

Notice that from equation (9), only two parameters are *structurally identifiable* (Walter and Pronzato, 1997). This means that in addition to d, one could also estimate η and C or η and ρ for instance.

To estimate d, η and C, (8) can be replaced by

$$\begin{bmatrix}\theta_3 \\ \theta_4\end{bmatrix} = s_t \begin{bmatrix}-1 & \rho H g \sin\theta - \rho H g \cos\theta \\ 0 & \tan\phi \rho_w g cos^2\theta\end{bmatrix} \begin{bmatrix}\bar{\eta}C/\eta \\ \bar{\eta}/\eta\end{bmatrix} \tag{16}$$

while for estimation of d, η and ρ, (8) can be replaced by

$$\begin{bmatrix}\theta_5 \\ \theta_6\end{bmatrix} = s_t \begin{bmatrix}Hg(\sin\theta - \cos\theta\tan\phi) & -C \\ 0 & \tan\phi\rho_w g cos^2\theta\end{bmatrix} \begin{bmatrix}\bar{\eta}\rho/\eta \\ \bar{\eta}/\eta\end{bmatrix}. \tag{17}$$

Notice also, still from (9), that actual identification of the parameters needs enough excitation (Besançon, 2007), and that when $w_t(t)$ lies below w_t^{crit}, identifiability is lost.

4. ILLUSTRATIVE EXAMPLES

4.1 Synthetic test case

To validate the effectiveness of our approach, a measured displacement profile d_{mea}^k is generated synthetically by solving system equations (6). The parameter values used for the simulation are summarized in Table 1. The water table height time-series is assumed to be sinusoidal in the simulations, representing seasonal variation. This water table height profile crosses w_t^{crit} calculated using (4). Simulated synthetic displacement measurement (with signal to noise ratio $40db$ white Gaussian noise) and water table profile are shown in Fig. 2.

Table 1. Parameter values (Synthetic test case)

Parameters	**Value**	**Unit**
Initial slide block displacement, d_0	0	m
Slide block thickness, H	2	m
Average inclination angle, θ	12	deg
Shear zone thickness, s_t	0.01	m
Acceleration due to gravity, g	9.8	m/s^2
Pore water density, ρ_w	1000	kg/m^3
Cohesion, C	1200	Pa
Slide block mass density, ρ	1600	kg/m^3
Time step, dt	3600	sec
Critical water table height, w_t^{crit}	1.55	m
Friction angle, ϕ	18	deg
Viscosity, η	10^8, 5×10^7	$Pa.s$

The proposed approach is utilized to estimate d, η, ϕ, and w_t^{crit} assuming all other parameters are known (Table 1). Initial states and scaling factor used in the simulation are introduced in Table 2. Note that, $\hat{\theta}_{10}$ and $\hat{\theta}_{20}$ are calculted using (8) with η_0 and ϕ_0 equals to 2×10^8 $Pa.s$ and 15 deg, respectively. A convergence in state

and paramater estimates can be seen in Fig. 3, Fig. 4, Fig. 5, Fig. 6, and Fig. 7 respectively. In practice some of the parameter values change with time. In order to take such a situation into consideration, a step change in viscosity η is introduced. This change in parameter value and its corresponding estimate can be seen in Fig. 5. In simulation results, it is observed that intial convergence time is two days and for the next change in parameter value convegence time is three days.

Table 2. Initial states/Scaling factor/Filter coefficients

State/Time step/Scaling fector	Value
Scaling factor,$\bar{\eta}$	10^8
Initial displacement,$\hat{d}_0$	0.01 m
Initial state,$\hat{\theta}_{10}$	-24.15
Initial state,$\hat{\theta}_{20}$	20.92
Initial state estimation error auto-covariance,P_0	$10^3 \times I_{3\times3}$
Process noise auto-covariance matrix,Q	$10^{-11} \times I_{3\times3}$
Measurement noise auto-covariance matrix,R	10^{-9}
Process noise gain matrix,G	$I_{3\times3}$

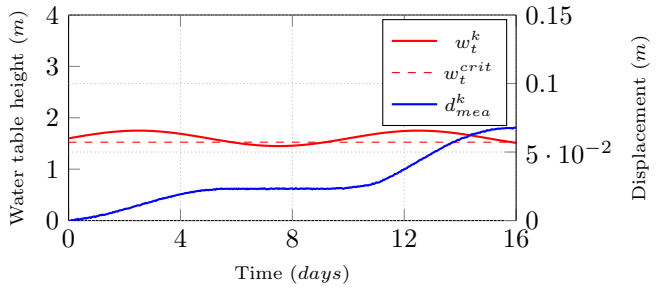

Fig. 2. Synthetic displacement measurement d_{mea}^k and water table height time-series w_t^k

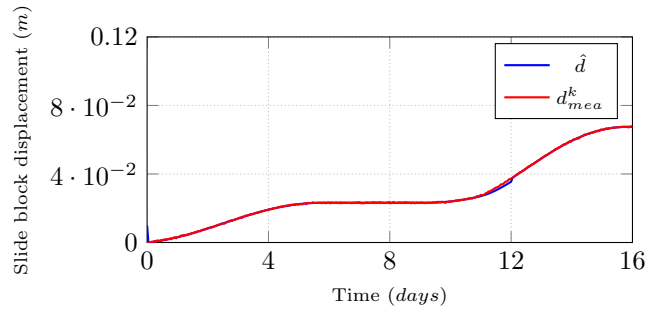

Fig. 3. Time evolution of state estimate $\hat{d}$

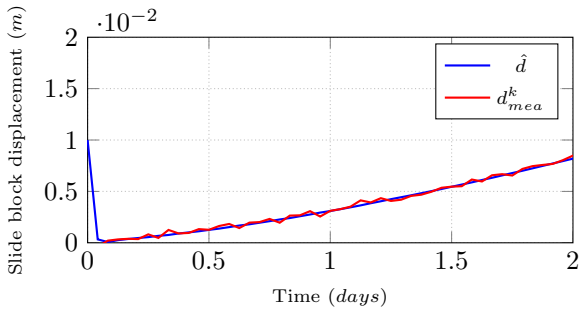

Fig. 4. Time evolution of state estimate $\hat{d}$ (Zoomed-in)

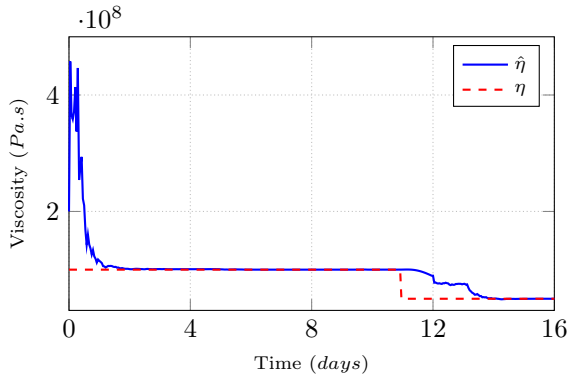

Fig. 5. Time evolution of parameter estimate $\hat{\eta}$

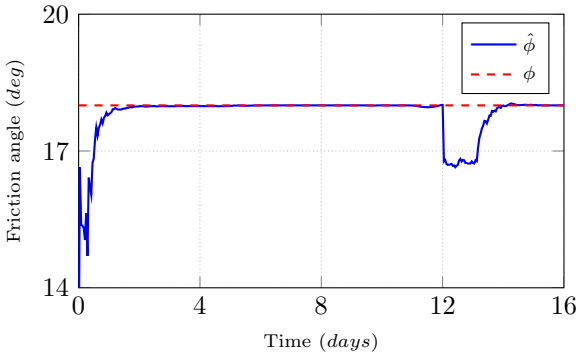

Fig. 6. Time evolution of parameter estimate $\hat{\phi}$

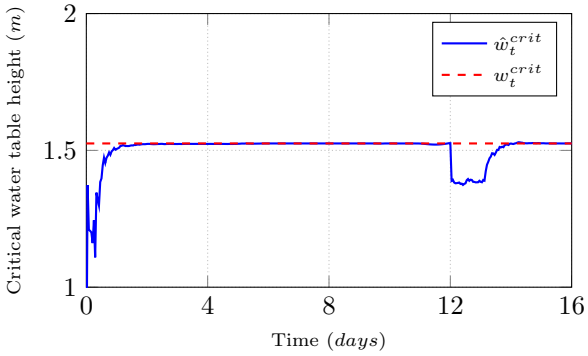

Fig. 7. Time evolution of parameter estimate $\hat{w}_t^{crit}$

4.2 The Super-Sauze landslide

As a second example, let us consider the case of an actual landslide. The Super-Sauze landslide is situated in the French South Alpes. To apply the proposed estimation strategy, displacement d_{mea}^k and pore water pressure p^k data are taken from (Bernardie et al., 2014). This data corresponds to one of the most active parts of the landslide for a period of high groundwater level from 07/05/1999 to 23/05/1999 (16 days), as shown in Fig. 8. At that position (location B_2), displacement and pore water pressure are measured by a wire extensometer and piezometer, respectively. In the proposed scheme, water table height time-series w_t^k is required as an input, which is reconstructed from p^k as follows (2)

$$w_t^k = p^k / \left(\rho_w g \cos^2\theta\right) \tag{18}$$

The known parameter values (Bernardie et al., 2014) are indicated in Table 3. Here, the value of ρ is chosen to be the saturated soil density (Malet et al., 2005) as the slide block is close to the full saturation level (Fig. 8).

Table 3. Parameter values (Super-Sauze)

Parameters	Value	Unit
Slide block thickness, H	9	m
Average inclination angle, θ	25	deg
Shear zone thickness, s_t	0.2	m
Acceleration due to gravity, g	9.8	m/s^2
Pore water density, ρ_w	1000	kg/m^3
Cohesion, C	14000	Pa
Slide block mass density, ρ	$1700 - 2140$	kg/m^3

The proposed scheme for estimation of displacement $\hat{d}$, friction angle $\hat{\phi}$ and viscosity $\hat{\eta}$ is performed with initial states, time step and scaling factor given in Table 4. Note that, $\hat{\theta}_{10}$ and $\hat{\theta}_{20}$ are calculted using (8) with initial viscosity η_0 and friction angle ϕ_0 equals to 10^8 $Pa.s$ and 35 deg (assumed), respectively. The state and paramater estimates are shown in Fig. 9, Fig. 10, Fig. 11, Fig. 12, and Fig. 13 respectively. Here, simulations are performed twice assuming the lower ($\rho = 1700$) and upper value ($\rho = 2140$) of the soil density (Table 3). It is observed that frictional angle ϕ stays constant (Fig. 12) ($33°/36.7°$) while viscosity η changes with time (Fig. 11). For first 9 days viscosity is nearly constant ($1.15\times10^8/8.7\times10^7$ $Pa.s$) then it changes to $1.2 \times 10^8/9.2 \times 10^7$ $Pa.s$ till day 12.5 and finally it stablizes to $1.3 \times 10^8/1 \times 10^8$ $Pa.s$. As mentioned earlier, the available data is for a period of high groundwater level therefore, w_t^k is always greater than $\hat{w}_t^{crit}$ (see in Fig. 13).

Table 4. Initial state/Time step/Scaling factor/Filter coefficients

State/Time step/Scaling fector	Value
Time step,dt	8640 sec
Scaling factor,$\bar{\eta}$	10^8
Initial displacement,$\hat{d}_0$	0.5 m
Initial state,$\hat{\theta}_{10}$	-8.89×10^3
Initial state,$\hat{\theta}_{20}$	1.17×10^3
Initial state estimation error auto-covariance,P_0	$10^3 \times I_{3\times3}$
Process noise auto-covariance matrix,Q	$10^{-11} \times I_{3\times3}$
Measurement noise auto-covariance matrix,R	10^{-9}
Process noise gain matrix,G	$I_{3\times3}$

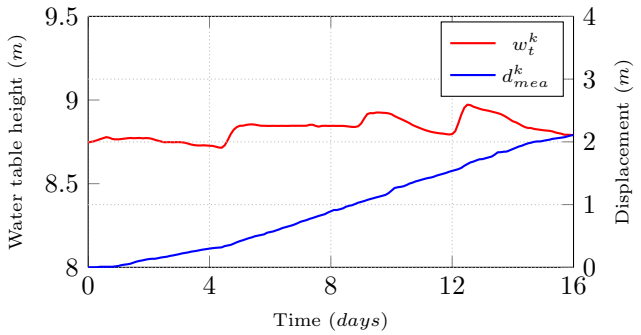

Fig. 8. The Super-Sauze landslide data from the literature: Displacement measurement d_{mea}^k and water table height time-series w_t^k (Bernardie et al., 2014)

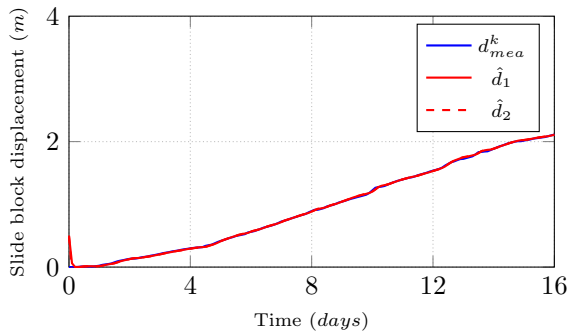

Fig. 9. Time evolution of state estimate $\hat{d}_1$ ($\rho = 1700$ kg/m^3) and $\hat{d}_2$ ($\rho = 2140$ kg/m^3)

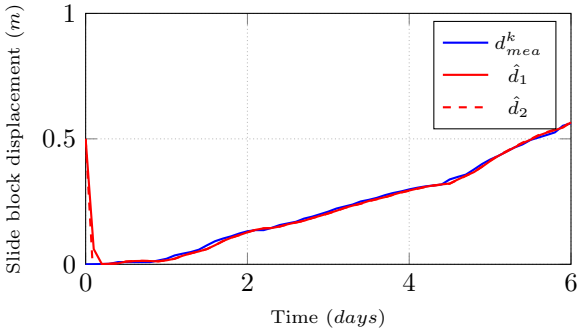

Fig. 10. Time evolution of state estimate $\hat{d}_1$ ($\rho = 1700$ kg/m^3) and $\hat{d}_2$ ($\rho = 2140$ kg/m^3) (Zoomed-in)

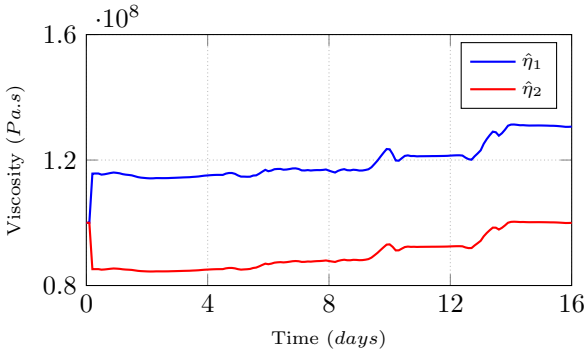

Fig. 11. Time evolution of parameter estimate $\hat{\eta}_1$ ($\rho = 1700$ kg/m^3) and $\hat{\eta}_2$ ($\rho = 2140$ kg/m^3)

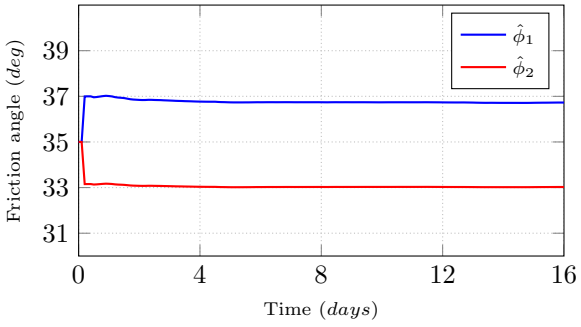

Fig. 12. Time evolution of parameter estimate $\hat{\phi}_1$ ($\rho = 1700$ kg/m^3) and $\hat{\phi}_2$ ($\rho = 2140$ kg/m^3)

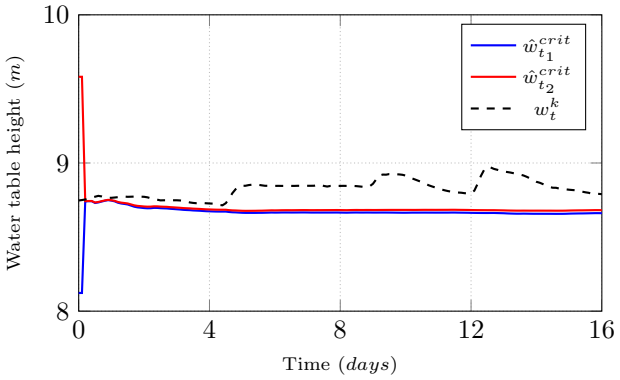

Fig. 13. Time evolution of parameter estimate $\hat{w}_{t_1}^{crit}$ ($\rho = 1700\ kg/m^3$),$\hat{w}_{t_2}^{crit}$ ($\rho = 2140\ kg/m^3$) and w_t^k

5. CONCLUSION

This paper employed a Kalman filter for state and parameter estimation of landslides on the synthetic test case and Super-Sauze landslide data from the literature. Firstly, we considered the landslide model depicting a landslide behavior described by an Ordinary Differential Equation (ODE). Secondly, the model is simplified to utilize the Kalman filter approach for information reconstruction, i.e., estimation of displacement and material properties (friction angle and viscosity) of landslides under investigation. In the simulation result for the Super-Sauze case (with real measurements), it is observed that friction angle almost remains constant while viscosity varies significantly through time.

A future direction for work will be to utilize the proposed approach for different landslides with extended time horizon data, which could comprise low groundwater level, i.e., less than critical water table height.

REFERENCES

Anderson, B. and Moore, J. (1979). *Optimal Filtering*. Prentice-Hall.

Atkinson, D.J., Acarnley, P.P., and Finch, J.W. (1991). Observers for induction motor state and parameter estimation. *IEEE Transactions on Industry Applications*, 27(6), 1119–1127.

Bernardie, S., Desramaut, N., Malet, J., Maxime, G., and Grandjean, G. (2014). Prediction of changes in landslide rates induced by rainfall. *Landslides*, 12. doi: 10.1007/s10346-014-0495-8.

Besançon, G. (2007). *Nonlinear observers and applications*. Springer.

Corominas, J., Moya, J., Ledesma, A., Lloret, A., and Gili, J. (2005). Prediction of ground displacements and velocities from groundwater level changes at the Vallcebre landslide (Eastern Pyrenees, Spain). *Landslides*, 2, 83–96. doi:10.1007/s10346-005-0049-1.

Fiolleau, S., Jongmans, D., Bivre, G., Chambon, G., Baillet, L., and Vial, B. (2020). Seismic characterization of a clay-block rupture in Harmalire landslide, French Western Alps. *Geophys J Int*, 221(3), 1777–1788. URL `https://doi.org/10.1093/gji/ggaa050`.

Guzzetti, F., Peruccacci, S., Rossi, M., and Stark, C.P. (2007). Rainfall thresholds for the initiation of landslides in central and southern Europe. *Meteorology and Atmospheric Physics*, 98(3), 239–267. URL `https://doi.org/10.1007/s00703-007-0262-7`.

Herrera, G., Fernandez-Merodo, J.A., Mulas, J., Pastor, M., Luzi, G., and Monserrat, O. (2013). A landslide forecasting model using ground based SAR data: The Portalet case study. *Engineering Geology*, 105, 220–230. doi:10.1016/j.enggeo.2009.02.009.

Hutchinson, J.N. (1986). A sliding-consolidation model for flow slides. *Canadian Geotechnical Journal*, 23(2), 115–126. doi:10.1139/t86-021.

Iverson, R. (2005). Regulation of landslide motion by dilatancy and pore pressure feedback. *J. Geophys. Res*, 110. doi:10.1029/2004JF000268.

Krøgli, I.K., Devoli, G., Colleuille, H., Boje, S., Sund, M., and Engen, I.K. (2018). The Norwegian forecasting and warning service for rainfall- and snowmelt-induced landslides. *Nat. Hazards Earth Syst. Sci.*, 18(5), 1427–1450. doi:10.5194/nhess-18-1427-2018.

Malet, J.P., Laigle, D., Rematre, A., and Maquaire, O. (2005). Triggering conditions and mobility of debris flows associated to complex earthflows. *Geomorphological hazard and human impact in mountain environments*, 66(1), 215–235.

Meng, J., Boukhnifer, M., Diallo, D., and Wang, T. (2020). A New Cascaded Framework for Lithium-Ion Battery State and Parameter Estimation. *Applied Sciences*, 10(3), 1009.

Mishra, M., Besançon, G., Chambon, G., and Baillet, L. (2020a). Observer design for state and parameter estimation in a landslide model. *IFAC-PapersOnLine*, 53(2), 16709–16714. doi: https://doi.org/10.1016/j.ifacol.2020.12.1116. 21th IFAC World Congress.

Mishra, M., Besançon, G., Chambon, G., and Baillet, L. (2020b). Optimal parameter estimation in a landslide motion model using the adjoint method. In *2020 European Control Conference (ECC)*, 226–231. doi: 10.23919/ECC51009.2020.9143819.

Nyambod, E.M. (2010). Environmental Consequences of Rapid Urbanisation: Bamenda City, Cameroon. *Journal of Environmental Protection*, 1, 15–23. doi: 10.4236/jep.2010.11003.

Petley, D.N., Mantovani, F., Bulmer, M.H., and Zannoni, A. (2005). The use of surface monitoring data for the interpretation of landslide movement patterns. *Geomorphological hazard and human impact in mountain environments*, 66(1), 133–147.

Saatci, E. and Akan, A. (2009). Dual Kalman Filter based State-Parameter Estimation in Linear Lung Models. In *4th European Conference of the International Federation for Medical and Biological Engineering*, 272–275. Springer Berlin Heidelberg, Berlin, Heidelberg.

Ţiclea, A. and Besançon, G. (2006). Observer Scheme for State and Parameter Estimation in Asynchronous Motors with Application to Speed Control. *European Journal of Control*, 12(4), 400–412.

Ţiclea, A. and Besançon, G. (2009). State and parameter estimation via discrete-time exponential forgetting factor observer. In *15th IFAC Symposium on System Identification, SYSID*, 1370–1374. Saint Malo, France.

Walter, E. and Pronzato, L. (1997). *Identification of Parametric Models*. Springer.